Gluon correlations in the glasma

T. Lappi

Department of Physics, P.O. Box 35, 40014 University of Jyväskylä, Finland and Helsinki Institute of Physics, P.O. Box 64, 00014 University of Helsinki, Finland

The physics of the initial conditions of heavy ion collisions is dominated by the nonlinear gluonic interactions of QCD. These lead to the concepts of parton saturation and the Color Glass Condensate (CGC). We discuss recent progress in calculating multi-gluon correlations in this framework, prompted by the observation that these correlations are in fact easier to compute in a dense system (nucleus-nucleus) than a dilute one (proton-proton).

§1. Introduction

Bulk particle production in relativistic collisions around midrapidity originates from small x degrees of freedom, predominantly gluons, in the wavefunctions of the colliding hadrons or nuclei. Because of the $\ln 1/x$ enhancement of soft gluon bremsstrahlung this is a dense gluonic system. When the occupation numbers of gluonic states in the wavefunction become large enough, of the order of $1/\alpha_{\rm s}$, the nonlinear interaction part of the Yang-Mills Lagrangian becomes of the same order of magnitude as the free part. This leads to the concept of a transverse momentum scale $Q_{\rm s}$, the *saturation scale*, below which the system is dominated by nonlinear interactions. When the collision energy is high enough (x small enough), $Q_{\rm s} \gg \Lambda_{\rm QCD}$ and the coupling is weak: we are faced with a *nonperturbative* strongly interacting system with a *weak coupling constant*. On the other hand, the large occupation numbers mean that the system should behave as a *classical* field. This suggests a way of organizing calculations that differs from traditional perturbation theory. Instead of developing as a series of powers in gA_μ one wants to calculate the classical background field $A^\mu_{\rm cl.}$ and loop corrections (which are suppressed by powers of g) to all orders in $gA^\mu_{\rm cl.}$. The classical gluon field will then be radiated by the large x degrees of freedom, which are treated as effective classical color charges. They can be described as random color charges drawn from a classical probability distribution $W_y[\rho]$ that depends on the rapidity cutoff $y = \ln 1/x$ separating the large and small x degrees of freedom. The dependence of $W_y[\rho]$ on y is described by a Wilsonian renormalization group equation known by the acronym JIMWLK. This picture of the high energy wavefunction is referred to as the Color Glass condensate (CGC, for reviews see e.g.[1)]).

The role of $W_y[\rho]$ is analoguous to the conventional parton distribution function; it is a nonperturbative quantity whose dependence on one of the kinematical variables of the process is described by a weak coupling renormalization group equation. In the case of pdf's the appropriate degrees of freedom are individual partons with a definite momentum, whereas in the case of the CGC they are color charges resulting from interactions of many partons. The distributions $W_y[\rho]$ are, like pdf's, not (complex)

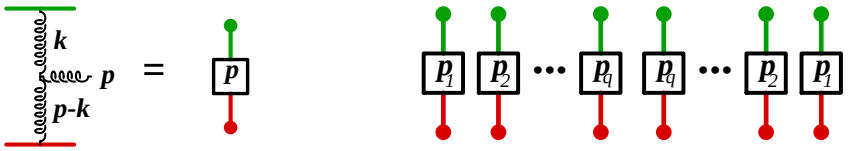

Fig. 1. Left: Building block, Lipatov vertex coupled to two sources. Right: combinatorics of the sources. The combinatorial problem is to connect the dots on the upper and lower side (left- and right moving sources) pairwise.

wavefunctions but real and can be interpreted as probability distributions. This is guaranteed by *factorization theorems*.[2] at large x and the process one is studying. Factorization can be understood as a statement that one has found the right set of degrees of freedom in which one can compute physical observables from only the diagonal elements of the density matrix of the incoming nuclei.

The term glasma[3] refers to the coherent, classical field configuration resulting from the collision of two objects described in the CGC framework. The glasma fields are initially longitudinal, whence the "glasma flux tube"[4),5] picture. More importantly for computing multigluon correlations, they are boost invariant (to leading order in the QCD coupling) and depend on the transverse coordinate with a characteristic correlation length $1/Q_\mathrm{s}$. There are several signals in the RHIC data[6),7] that point to strong correlations originating from the initial stage of the collision. The glasma fields provide a natural framework for understanding these effects, although much work is still left to do in understanding the interplay with purely geometrical effects from the fluctuating positions of the nucleons in the colliding nuclei.[8]

We shall first make some general observations on computing multigluon correlations in the glasma, arguing in Sec. 2 that they are in some sense simpler to compute in a collision of two dense, saturated nuclear wavefunctions than in the dilute limit. We shall then, in Sec. 3 discuss one application of these ideas to computing the multiplicity distribution of gluons in the collision before moving to the leading $\ln 1/x$ rapidity dependence of the correlation in Sec. 4. The application of these ideas to understanding correlations observed in the experimental data are discussed in Sec. 5.

§2. Multigluon correlations in the glasma

The gluon fields in the glasma are nonperturbatively strong, $A_\mu \sim 1/g$. This means that the gluon multiplicity is $N \sim 1/\alpha_\mathrm{s}$. For a fixed configuration of the classical color sources it is well known that the multiplicity distribution of produced gluons is Poissonian, i.e. $\langle N^2\rangle - \langle N\rangle^2 = \langle N\rangle$. In this case the correlations and fluctuations in the gluon multiplicity are all quantum effects that appear only starting from the one-loop level, i.e. suppressed by a power of the coupling constant α_s. The computation in the CGC framework does not end here, however. To calculate the moments of the gluon multiplicity distribution one must first calculate the gluon spectra for fixed configuration of the color charges ρ and then average over the probability distribution $W_y[\rho(\boldsymbol{x}_\perp)]$. For the nth moment of the multiplicity distribution,

i.e. an n-gluon correlation, the leading order result is

$$\left\langle \frac{\mathrm{d}N}{\mathrm{d}^3\boldsymbol{p}_1}\cdots\frac{\mathrm{d}N}{\mathrm{d}^3\boldsymbol{p}_n}\right\rangle = \left[\int_{[\rho]} W\big[\rho_1(y)\big]W\big[\rho_2(y)\big]\,\frac{\mathrm{d}N}{\mathrm{d}^3\boldsymbol{p}_1}\bigg|_{\mathrm{LO}}\cdots\frac{\mathrm{d}N}{\mathrm{d}^3\boldsymbol{p}_n}\bigg|_{\mathrm{LO}}\right], \qquad (2\cdot1)$$

where the subsrcipt "LO" refers to the single gluon spectrum evaluated from the classical field configuration corresponding to a fixed configuration of color charges. This averaging, even after the subsequent subtraction of the appropriate disconnected contributions, introduces a correlation already at the leading order in α_{s}, i.e. enhanced by an additional $1/\alpha_{\mathrm{s}}$ compared to the quantum correlations. A natural example is the negative binomial distribution that we shall discuss below, whose variance is $\langle N^2\rangle - \langle N\rangle^2 = \langle N\rangle^2/k + \langle N\rangle$. One must emphasize here that although these contributions arise as formally classical correlations in the effective theory that is the CGC, they are physically also quantum effects, where the weak coupling is compensated by a large logarithm of the energy that has been resummed into the probability distribution $W_y[\rho(\boldsymbol{x}_\perp)]$. In this sense the leading correlations are present already in the wavefunctions of the colliding objects.

§3. Multiplicity distribution

We can then apply this formalism to the calculation of the probability distribution of the number of gluons in the glasma.[9] We shall assume the "AA" power counting of sources ρ that are parametrically strong in g, but nevertheless work to the lowest nontrivial order in ρ. Formally this would correspond to a power counting $\rho \sim g^{\varepsilon-1}$ with a small $\epsilon > 0$. In this limit, as we have discussed, the dominant contributions to multiparticle correlations come from diagrams that are disconnected for fixed sources and become connected only after averaging over the color charge configurations. The corresponding two gluon correlation function was computed in Ref.[4] and generalized to a three gluons in Ref.[10] We shall here sketch the derivation[9] of the general n-gluon correlation in this simplified limit.

Working with the MV model Gaussian probability distribution

$$W[\rho] = \exp\left[-\int \mathrm{d}^2\boldsymbol{x}_\perp \frac{\rho^a(\boldsymbol{x}_\perp)\rho^a(\boldsymbol{x}_\perp)}{g^4\mu^2}\right] \qquad (3\cdot1)$$

computing the correlations and the multiplicity distribution in the linearized approximation is a simple combinatorial problem. Each gluon is produced from two Lipatov vertices (see fig. 1 left), one in the amplitude and the other in the complex conjugate. The combinatorial factor is obtained by counting the different ways of contracting the sources pairwise (see fig. 1 right). The dominant contributions are the ones that have, in the dilute limit, the strongest infrared divergence which is regulated by the transverse correlation scale of the problem, Q_{s}. When integrated over the momenta of the produced gluons one obtains the factorial moments of the multiplicity, which define the whole probability distribution. It can be expressed in terms of two parameters, the mean multiplicity $\bar{n}$, and a parameter k describing

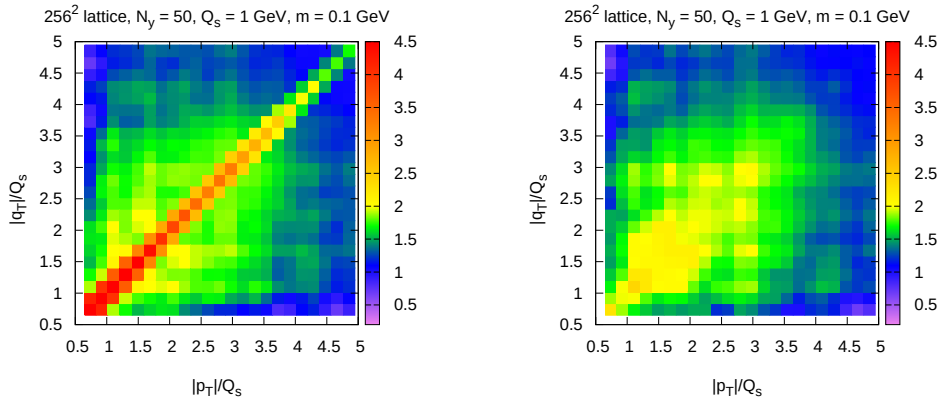

Fig. 2. Numerical evaluation of the two-gluon correlation strength in the MV model as a function of the two transverse momenta $p_\perp$ and $q_\perp$. Left: the correlation strength on the "near side" $|\varphi_p - \varphi_q| < \pi/2$, right: the "away side" $|\varphi_p - \varphi_q| > \pi/2$.

the width of the distribution. The result of the combinatorial exercise is that the qth factorial moment m_q (defined as $\langle N^q \rangle$ minus the corresponding disconnected contributions) is

$$m_q = (q-1)!\, k \left(\frac{\bar{n}}{k}\right)^q \quad \text{with} \quad k \approx \frac{({N_\mathrm{c}}^2 - 1) Q_\mathrm{s}^2 S_\perp}{2\pi} \quad \text{and} \quad \bar{n} = f_N \frac{1}{\alpha_\mathrm{s}} Q_\mathrm{s}^2 S_\perp. \quad (3{\cdot}2)$$

Here $S_\perp$ is the transverse area of the system. These moments define a *negative binomial* distribution (NBD) with parameters k and $\bar{n}$. The NBD has been known as a purely phenomenological observation in high energy hadron and nuclear collisions already for a long time. Also the numerical magnitude of the parameter k obtained from the saturation scale agrees very well with both pp and AA data.[11),12)]

In terms of the glasma flux tube picture this result has a natural interpretation. The transverse area of a typical flux tube is $1/Q_\mathrm{s}^2$, and thus there are $Q_\mathrm{s}^2 S_\perp = N_\mathrm{FT}$ independent ones. Each of these radiates particles independently into ${N_\mathrm{c}}^2 - 1$ color states in a Bose-Einstein distribution (see e.g.[13)]). A sum of $k \approx N_\mathrm{FT}({N_\mathrm{c}}^2 - 1)$ independent Bose-Einstein-distributions is precisely equivalent to a negative binomial distribution with parameter k.

This calculation predicts that the k parameter should increase with energy as $k \sim Q_\mathrm{s}^2 \sim \sqrt{s}^\lambda$. This is ideed true in the heavy ion data; k is reported to increase from $\sqrt{s} = A62$ GeV to $A200$ GeV in by the PHENIX collaboration.[12)] However, the interpretation of the heavy ion data is complicated by the purely geometrical fluctuations from the different impact parameters probed in one centrality bin.

The proton-proton collision system is much smaller and fluctuations at lower energies are still mostly dominated by the dilute edge of the collision system, which has a Poissonian nature (i.e. $k \to \infty$). Our calculation formally assumes $Q_\mathrm{s}^2 S_\perp \gg 1$, and we expect the growing behavior of k with energy to eventually take over at high enough energy. Since the fluctuations are more dominated by the edge region than the mean multiplicity, it is natural to expect this transition to a genuine high energy regime to be visible later in the fluctuations than it is in the average. At

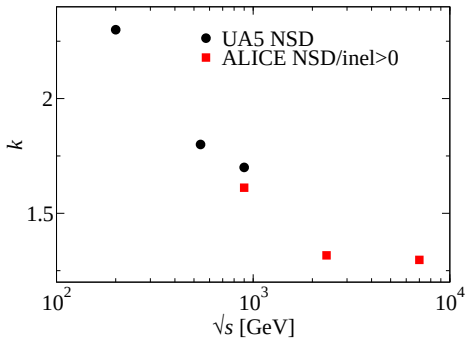

Fig. 3. The parameter k in pp collisions measured by the UA5,[11] and ALICE.[14] For UA5 the NBD fit is done by the experiment. The fit to ALICE data is done by us and does not take into account the correlated errors in the experimental data points.

LHC energies (see the data in Ref.[14]) the transition to an increasing k seems to be starting as shown in fig. 3.

§4. Rapidity dependence

The general discussion of Sec. 2 on the different nature of multigluon correlations in the "AA" case applies also to the rapidity dependence. Until now we have only been discussing gluon production in a rapidity interval smaller than $1/\alpha_{\rm s}$. For this we needed only the correlations between the color charges $\rho(\boldsymbol{x}_\perp)$ measured at this same rapidity. To understand the rapidity dependence of the correlations one needs also the correlation between color charges at different rapidities, $\langle \rho_y(\boldsymbol{x}_\perp)\rho_{y'}(\boldsymbol{y}_\perp)\rangle$. Also this information is contained in the JIMWLK renormalization group evolution, at least to leading $\ln 1/x$ accuracy.[15] An intuitive description of the resulting correlations is provided by the formulation of JIMWLK as a Langevin equation in the space of Wilson lines formed from the color charges. In this picture the evolution proceeds in individual trajectories along an increasing rapidity.

A first attempt of a realistic estimate of the rapidity dependence of two-gluon correlations is performed in Ref.[16] Evaluating the two gluon correlation in a dilute limit in a $k_\perp$-factorized approximation, but keeping the general structure resulting from the JIMWLK evolution leads to the following expression:

$$C(\boldsymbol{p},\boldsymbol{q}) = \frac{{\alpha_{\rm s}}^2}{16\pi^{10}}\frac{N_c^2(N_c^2-1)S_\perp}{{d_{\rm A}}^4\,{\boldsymbol{p}_\perp}^2\boldsymbol{q}_\perp^2}$$
$$\times\left\{\int \mathrm{d}^2\boldsymbol{k}_\perp \Phi^2_{A_1}(y_p,\boldsymbol{k}_\perp)\Phi_{A_2}(y_p,\boldsymbol{p}_\perp-\boldsymbol{k}_\perp)\Big[\Phi_{A_2}(y_q,\boldsymbol{q}_\perp+\boldsymbol{k}_\perp)+\Phi_{A_2}(y_q,\boldsymbol{q}_\perp-\boldsymbol{k}_\perp)\Big]\right.$$
$$\left.+\,\Phi^2_{A_2}(y_q,\boldsymbol{k}_\perp)\Phi_{A_1}(y_p,\boldsymbol{p}_\perp-\boldsymbol{k}_\perp)\Big[\Phi_{A_1}(y_q,\boldsymbol{q}_\perp+\boldsymbol{k}_\perp)+\Phi_{A_1}(y_q,\boldsymbol{q}_\perp-\boldsymbol{k}_\perp)\Big]\right\}. \quad (4\cdot1)$$

Note the very different structure of this correlation compared to one where the gluons would be produced from the same diagram for fixed sources. The two gluon correlation function is proportional to the product of *four* unintegrated gluon distri-

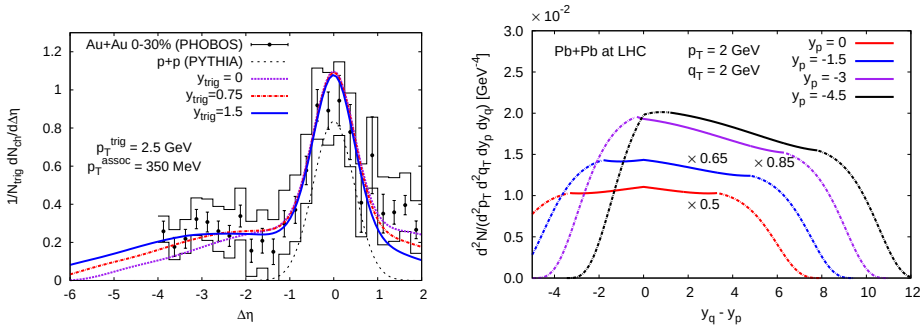

Fig. 4. Left: Comparison of a two-particle correlation computed using eq. (4·1) supplemented with a short-range correlation contribution from PYTHIA with PHOBOS data. Right: Rapidity correlation at LHC energies $k_\perp$-factorization approximation.

butions, with three of them evaluated at the rapidity of one of the produced gluons and only one at the other. This structure is a direct consequence of the nature of JIMWLK evolution.

§5. The ridge in nuclear and proton collisions

The "ridge" is a feature on the "near side" of the two particle correlation, around $\Delta\phi \approx 0$ azimuthal separation between the two particles. It extends up to high values of $\Delta\eta$, the pseudorapidity difference between the two particles. This feature was first seen in nucleus–nucleus collisions at RHIC.[17)–21)] The ridge was seen in high multiplicity (central) events in nucleus-nucleus collisions in Cu+Cu collisions at $\sqrt{s} = 62.4$ GeV and in Au+Au collisions at $\sqrt{s} = 200$ GeV. The STAR detector observed this correlation for both $p_\perp$-triggered[18)] and untriggered[17)] pair correlations in the whole STAR TPC acceptance of $\Delta\eta \leq 2$. The PHOBOS experiment[20)] observed the $p_\perp$-triggered correlation at much larger rapidity separations, initially up to $\Delta\eta \sim 4$, extended more recently[21)] to $\Delta\eta \sim 5$. The long range correlation structure disappears for lower multiplicity peripheral events in nucleus-nucleus collisions and are also absent in deuteron-gold and proton-proton "control" experiments at the same energies.

The "standard" glasma explanation[4)] of the azimuthal structure of the ridge relies on a collimation effect from radial flow combined with the long range rapidity correlation from the boost invariant color fields. The correlation computed from eq. (4·1) is compared to PHOBOS data in fig. 4. The $k_\perp$-factorized approximation gives a very inaccurate description of the gluon spectrum in the transverse momentum regime $p_\perp \sim Q_\mathrm{s}$ where the bulk of the particles are produced.[22)] Equation (4·1) has also been derived in the approximation, true only in the linearized case, that the unequal rapidity correlation of two color charge densities is equal to the unintegrated gluon distribution at the smaller one of these rapidities. As of yet there is no calculation of how much this approximation is violated in the full JIMWLK evolution (see, however,[23)]). The results presented in fig. 4 are therefore not the final word on the subject, alhough it is reassuring that such a simple approximation

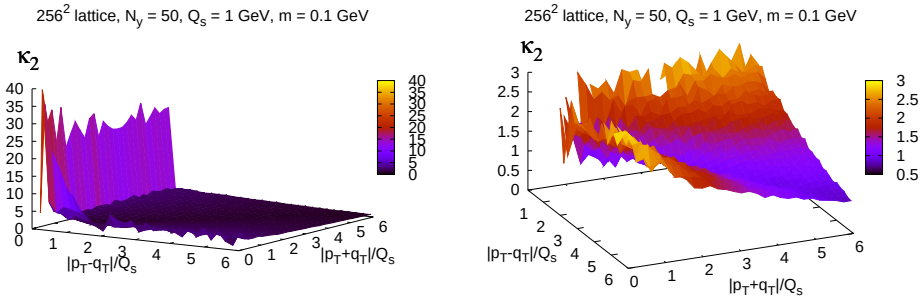

Fig. 5. Two-gluon correlation strength in the MV model. Both figures show the same data; the large delta function peaks have been removed from the one on the right to illustrate the structure in the rest of phase space.

seems to agree rather well with the experimental result. A numerical evaluation[24] of the second moment of the distribution, parametrized in terms of

$$\kappa_2(\boldsymbol{p}_\perp, \boldsymbol{q}_\perp) = Q_s^2 S_\perp \left(\frac{\mathrm{d}^2 N}{\mathrm{d}^2\boldsymbol{p}_\perp \mathrm{d}^2\boldsymbol{q}_\perp} - \frac{\mathrm{d}N}{\mathrm{d}^2\boldsymbol{p}_\perp} \frac{\mathrm{d}N}{\mathrm{d}^2\boldsymbol{q}_\perp} \right) \Big/ \frac{\mathrm{d}N}{\mathrm{d}^2\boldsymbol{p}_\perp} \frac{\mathrm{d}N}{\mathrm{d}^2\boldsymbol{q}_\perp} \tag{5·1}$$

is shown in Fig. 2. It confirms the expectations of Ref.[9] on the magnitude of the correlation. In contrast to the approximation made in Ref.[9] there is, however, some dependence on the momenta $\boldsymbol{p}_\perp, \boldsymbol{q}_\perp$, which is crucial for the discussion of the correlation in smaller systems where transverse flow is smaller or absent.

More recently the CMS collaboration has reported the observation of a "ridge" structure also in proton-proton collisions.[25] The ridge is seen only in the moderate $p_\perp, q_\perp$ range and systematically vanishes for $p_\perp, q_\perp \lesssim 1$ GeV and $p_\perp, q_\perp \gtrsim 3$ GeV. Although the explanation in terms of the collimating effect of the transverse flow is most likely present to some degree in high multiplicity proton-proton collisions at LHC energies, this observation points to a ridge-like effect being present already in the initial scattering process. This is indeed the picture resulting from the correlations in the glasma.

In terms of the $k_\perp$-factorized assumption (4·1) the CMS data was recently discussed in Ref.[26] The dependence of the CMS ridge on transverse momentum was found to qualitatively agree with the CMS result. In the full nonperturbative calculation this same collimation effect already in the initial stage is visible in fig. 5, where the correlation is plotted as a function of $|\boldsymbol{p}_\perp - \boldsymbol{q}_\perp|$ and $|\boldsymbol{p}_\perp + \boldsymbol{q}_\perp|$. The production of gluons from a coherent classical field results in an enhanced near side correlation for momenta $\boldsymbol{p}_\perp$ and $\boldsymbol{q}$ that are close to parallel, even in the absence of transverse flow.

§6. Conclusion

Most experimental observables do not probe the glasma initial state of directly, because the system goes through a complicated time evolution before the hadronization stage. A good candidate for an experimental probe giving direct access to the

initial state is provided by different kinds of correlation measurements. These have indeed been a focus of both experimental and theoretical activity recently. We have argued here that the glasma picture of the initial stages of a heavy ion collision is the natural framework to understand the origin of these correlations.

Acknowledgements

The author thanks the Yukawa Institute of Theoretical Physics t Kyoto University for hospitality and support during YIPQS Workshop "High energy strong interactions 2010." The author is supported by the Academy of Finland, contract 126604.

References

1) E. Iancu and R. Venugopalan, The color glass condensate and high energy scattering in QCD, in *Quark gluon plasma*, edited by R. Hwa and X. N. Wang, World Scientific, 2003, arXiv:hep-ph/0303204; H. Weigert, Prog. Part. Nucl. Phys. **55**, 461 (2005), [arXiv:hep-ph/0501087]; F. Gelis, E. Iancu, J. Jalilian-Marian and R. Venugopalan, arXiv:1002.0333 [hep-ph]; T. Lappi, arXiv:1003.1852 [hep-ph].
2) F. Gelis, T. Lappi and R. Venugopalan, Phys. Rev. **D78**, 054019 (2008), [arXiv:0804.2630 [hep-ph]]; F. Gelis, T. Lappi and R. Venugopalan, Phys. Rev. **D78**, 054020 (2008), [arXiv:0807.1306 [hep-ph]].
3) T. Lappi and L. McLerran, Nucl. Phys. **A772**, 200 (2006), [arXiv:hep-ph/0602189].
4) A. Dumitru, F. Gelis, L. McLerran and R. Venugopalan, Nucl. Phys. **A810**, 91 (2008), [arXiv:0804.3858 [hep-ph]].
5) S. Gavin, L. McLerran and G. Moschelli, Phys. Rev. **C79**, 051902 (2009), [arXiv:0806.4718 [nucl-th]].
6) J. Putschke, J. Phys. **G34**, S679 (2007), [arXiv:nucl-ex/0701074]; STAR, M. Daugherity, J. Phys. **G35**, 104090 (2008), [arXiv:0806.2121 [nucl-ex]]; PHOBOS, B. Alver *et al.*, J. Phys. **G35**, 104080 (2008), [arXiv:0804.3038 [nucl-ex]].
7) STAR, B. I. Abelev *et al.*, Phys. Rev. Lett **103**, 172301 (2009), [arXiv:0905.0237 [nucl-ex]].
8) T. Lappi and L. McLerran, Nucl. Phys. **A832**, 330 (2010), [arXiv:0909.0428 [hep-ph]].
9) F. Gelis, T. Lappi and L. McLerran, Nucl. Phys. **A828**, 149 (2009), [arXiv:0905.3234 [hep-ph]].
10) K. Dusling, D. Fernandez-Fraile and R. Venugopalan, Nucl. Phys. **A828**, 161 (2009), [arXiv:0902.4435 [nucl-th]].
11) UA5, G. J. Alner *et al.*, Phys. Lett. **B160**, 193 (1985); UA5, R. E. Ansorge *et al.*, Z. Phys. **C37**, 191 (1988).
12) PHENIX, A. Adare *et al.*, Phys. Rev. **C78**, 044902 (2008), [arXiv:0805.1521 [nucl-ex]].
13) K. Fukushima, F. Gelis and T. Lappi, Nucl. Phys. **A831**, 184 (2009), [arXiv:0907.4793 [hep-ph]].
14) ALICE, K. Aamodt *et al.*, Eur. Phys. J. **C68**, 89 (2010), [arXiv:1004.3034 [hep-ex]]; ALICE, K. Aamodt *et al.*, Eur. Phys. J. **C68**, 345 (2010), [arXiv:1004.3514 [hep-ex]].
15) F. Gelis, T. Lappi and R. Venugopalan, Phys. Rev. **D79**, 094017 (2008), [arXiv:0810.4829 [hep-ph]]; T. Lappi, Acta Phys. Polon. **B40**, 1997 (2009), [arXiv:0904.1670 [hep-ph]].
16) K. Dusling, F. Gelis, T. Lappi and R. Venugopalan, Nucl. Phys. **A836**, 159 (2010), [arXiv:0911.2720 [hep-ph]].
17) STAR, J. Adams *et al.*, Phys. Rev. **C73**, 064907 (2006), [arXiv:nucl-ex/0411003].
18) STAR, J. Adams *et al.*, Phys. Rev. Lett. **95**, 152301 (2005), [arXiv:nucl-ex/0501016].
19) PHENIX, A. Adare *et al.*, Phys. Rev. **C78**, 014901 (2008), [arXiv:0801.4545 [nucl-ex]].
20) PHOBOS, B. Alver *et al.*, Phys. Rev. Lett. **104**, 062301 (2010), [arXiv:0903.2811 [nucl-ex]].
21) PHOBOS, B. Alver *et al.*, Phys. Rev. **C81**, 034915 (2010), [arXiv:1002.0534 [nucl-ex]].
22) J. P. Blaizot, T. Lappi and Y. Mehtar-Tani, Nucl. Phys. **A846**, 63 (2010), [arXiv:1005.0955 [hep-ph]].
23) A. Dumitru and J. Jalilian-Marian, Phys. Rev. **D81**, 094015 (2010), [arXiv:1001.4820 [hep-ph]].
24) T. Lappi, S. Srednyak and R. Venugopalan, JHEP **01**, 066 (2010), [arXiv:0911.2068 [hep-ph]].
25) CMS, V. Khachatryan *et al.*, JHEP **09**, 091 (2010), [arXiv:1009.4122 [hep-ex]].
26) A. Dumitru *et al.*, arXiv:1009.5295 [hep-ph].